Thermal coefficients of the methyl groups within ubiquitin

T. Michael Sabo,[1] Davood Bakhtiari,[1] Korvin F. A. Walter,[1] Robert L. McFeeters,[2] Karin Giller,[1] Stefan Becker,[1] Christian Griesinger,[1]* and Donghan Lee[1]*

[1]Department of NMR-based Structural Biology, Max-Planck Institute for Biophysical Chemistry, Göttingen 37077, Germany
[2]Department of Chemistry, University of Alabama in Huntsville, Huntsville, Alabama 35899

Received 13 December 2011; Revised 6 February 2012; Accepted 7 February 2012
DOI: 10.1002/pro.2045
Published online 14 February 2012 proteinscience.org

Abstract: Physiological processes such as protein folding and molecular recognition are intricately linked to their dynamic signature, which is reflected in their thermal coefficient. In addition, the local conformational entropy is directly related to the degrees of freedom, which each residue possesses within its conformational space. Therefore, the temperature dependence of the local conformational entropy may provide insight into understanding how local dynamics may affect the stability of proteins. Here, we analyze the temperature dependence of internal methyl group dynamics derived from the cross-correlated relaxation between dipolar couplings of two CH bonds within ubiquitin. Spanning a temperature range from 275 to 308 K, internal methyl group dynamics tend to increase with increasing temperature, which translates to a general increase in local conformational entropy. With this data measured over multiple temperatures, the thermal coefficient of the methyl group order parameter, the characteristic thermal coefficient, and the local heat capacity were obtained. By analyzing the distribution of methyl group thermal coefficients within ubiquitin, we found that the N-terminal region has relatively high thermostability. These results indicate that methyl groups contribute quite appreciably to the total heat capacity of ubiquitin through the regulation of local conformational entropy.

Keywords: NMR; methyl group dynamics; cross-correlated relaxation; thermal coefficients; protein stability; ubiquitin

Introduction

The intricate relationship between structure, function, and dynamics strongly influences such fundamental physiological processes as protein folding, molecular recognition, and thermal stability. All of these processes occur with concomitant changes in the thermodynamic parameters of the system, specifically the enthalpy (H) and the entropy (S). The linkage between the temperature dependence of H and S is expressed by the heat capacity (C_p).[1,2] Contributions to the C_p of a protein include hydration of solvent exposed surface area, covalent bonds, electrostatic interactions, and hydrogen bonds. In addition, the local conformational entropy (S_{conf}) of residues within a protein must also be considered. The term S_{conf} is directly related to the degrees of freedom each residue possesses within the three-dimensional protein structure. Therefore, an understanding of the dependence of S_{conf} on temperature, encapsulated by C_p, yields insight into the role local dynamics play in controlling the stability of proteins.

Additional Supporting Information may be found in the online version of this article.

T. Michael Sabo and Davood Bakhtiari contributed equally to this work.

Grant sponsor: Max Planck Society; Grant sponsor: European Research Council; Grant number: 233227; Grant sponsor: Alexander von Humboldt Foundation

*Correspondence to: Christian Griesinger, Department of NMR-based Structural Biology, Max-Planck Institute for Biophysical Chemistry, Am Fassberg 11, Göttingen 37077, Germany. E-mail: cigr@nmr.mpibpc.mpg.de or Donghan Lee, Department of NMR-based Structural Biology, Max-Planck Institute for Biophysical Chemistry, Am Fassberg 11, Göttingen 37077, Germany. E-mail: dole@nmr.mpibpc.mpg.de

Nuclear magnetic resonance (NMR) spectroscopy provides a potent tool for characterizing such local dynamics with atomic resolution on multiple time-scales. Analysis of spin-lattice relaxation (T_1), spin-spin relaxation (T_2), and steady-state nuclear Overhauser enhancements[3] with the "model free" formalism introduced by Lipari and Szabo allows the extraction of a general order parameter (S^2) that describes the amplitude of the individual bond vector motions on the ps to ns time-scale.[4,5] The relationship between S^2 and S_{conf} results from the dependence of both parameters on the population distribution of bond vector orientations.[6–8] By measuring relaxation data at multiple temperatures, the temperature dependence of S^2 ultimately provides the local C_p for each bond vector.[9–13]

An important probe ideally suited for providing fundamental insight into protein folding, stability, and recognition are methyl groups. Located primarily within the hydrophobic core of proteins, methyl groups are typically quite numerous, well dispersed throughout the core, and possess a wide variety of motional amplitudes.[9,14–16] For these reasons, determining the methyl group order parameters (S^2_{axis}) provides an avenue for understanding how methyl dynamics on the ps to ns time scale are related to protein stability. To obtain S^2_{axis}, typically the methyl groups in a protein are deuterated (—CH_2D or —CHD_2) for performing deuterium relaxation measurements.[17–19] An alternative to this approach is to utilize cross-correlated relaxation (CCR) between dipolar couplings of two CH bonds (σ) in the methyl group for extracting S^2_{axis}.[20,21]

An inherent advantage to determining S^2_{axis} from σ versus deuterium relaxation is the savings in measurement time, especially important for measuring S^2_{axis} at many different temperatures. In the past, S^2_{axis} calculated at one temperature point with deuterium relaxation studies could take up to 1 week due to the requirement of data being recorded at two fields.[17] Recent advances in determining S^2_{axis} from the measurement of five relaxation rates for —CH_2D[19] and four relaxation rates for —CHD_2[18] has effectively reduced the amount of time necessary to obtain the same information to ~1 day. Yet, S^2_{axis} derived from σ can require as little as 1 h of measurement time and, thus, is ideally suited for studying the temperature dependence of S^2_{axis}.

Here, we report the temperature dependence of the methyl group order parameters derived from the CCR between dipolar couplings of two CH bonds in ubiquitin. From these measurements, we calculate the thermal coefficients characterizing this temperature dependence, specifically the characteristic thermal coefficient Λ and the local heat capacity C_p. Furthermore, we analyze the distribution of methyl group thermal coefficients within ubiquitin, illustrating the relatively high thermostability of the N-terminal region of this protein.

Results and Discussion

Methyl group CCR

Two dimensional constant time ^{13}C, ^{1}H HSQC measurements without decoupling of ^{1}H during ^{13}C-chemical shift evolution leads to splitting of the methyl group ^{13}C signal into a quartet.[22,23] The peaks in the quartet are separated by the J-coupling constant for C—H bonds in a methyl group (J_{CH} = 125 Hz). The quartet represents the four coherences of $C_x H_{1\alpha} H_{2\alpha} H_{3\alpha}$, $C_x(H_{1\beta} H_{2\alpha} H_{3\alpha} + H_{1\alpha} H_{2\beta} H_{3\alpha} + H_{1\alpha} H_{2\alpha} H_{3\beta})$, $C_x(H_{1\beta} H_{2\beta} H_{3\alpha} + H_{1\alpha} H_{2\beta} H_{3\beta} + H_{1\beta} H_{2\alpha} H_{3\beta})$, and $C_x(H_{1\beta} H_{2\beta} H_{3\beta})$ and their intensity ratio ($I_{\alpha^3} : I_{\alpha^2\beta} : I_{\alpha\beta^2} : I_{\beta^3}$) is 3:1:1:3 in the absence of relaxation.[22,24] With the contribution of the transverse relaxation rate (R_{2,I_i}),[25] the intensities can be expressed as:

$$\begin{aligned} I_{\alpha^3} &\propto 3e^{-R_{2,I_{\alpha^3}}\Delta} \\ I_{\alpha^2\beta} &\propto e^{-R_{2,I_{\alpha^2\beta}}\Delta} \\ I_{\alpha\beta^2} &\propto e^{-R_{2,I_{\alpha\beta^2}}\Delta}, \\ I_{\beta^3} &\propto 3e^{-R_{2,I_{\beta^3}}\Delta} \end{aligned} \tag{1}$$

where Δ is the length of the constant time period.

By considering the dipolar coupling and chemical shift anisotropy (CSA), R_{2,I_i} can be expressed as: [20,25]

$$\begin{aligned} R_{2,I_{\alpha^3}} &= \lambda + 3\sigma + 2\eta \\ R_{2,I_{\alpha^2\beta}} &= \lambda - \sigma + \frac{2}{3}\eta \\ R_{2,I_{\alpha\beta^2}} &= \lambda - \sigma - \frac{2}{3}\eta \\ R_{2,I_{\beta^3}} &= \lambda + 3\sigma - 2\eta \end{aligned} \tag{2}$$

where λ is the rate of the autorelaxation and σ and η are the rate of the CCR between dipolar couplings of two CH bonds and between dipolar coupling of CH and CSA of the ^{13}C nucleus, respectively. Thus, the CCR rate between dipolar couplings of two CH bonds can be determined experimentally from the intensities of the quartet,[20]

$$\sigma_{obs} = \frac{1}{8\Delta} \ln \frac{9 I_{\alpha^2\beta} I_{\alpha\beta^2}}{I_{\alpha^3} I_{\beta^3}}. \tag{3}$$

Here, we report the temperature dependence of σ_{obs} for the methyl groups of uniformly ^{15}N, ^{13}C-labeled human ubiquitin extracted from a series of 2D constant time ^{13}C, ^{1}H HSQC measurements at fourteen temperatures: 275, 278, 281, 283, 286, 288, 291, 293, 296, 298, 301, 303, 305, and 308 K. Ubiquitin possesses 50 methyl groups residing in 30 residues.

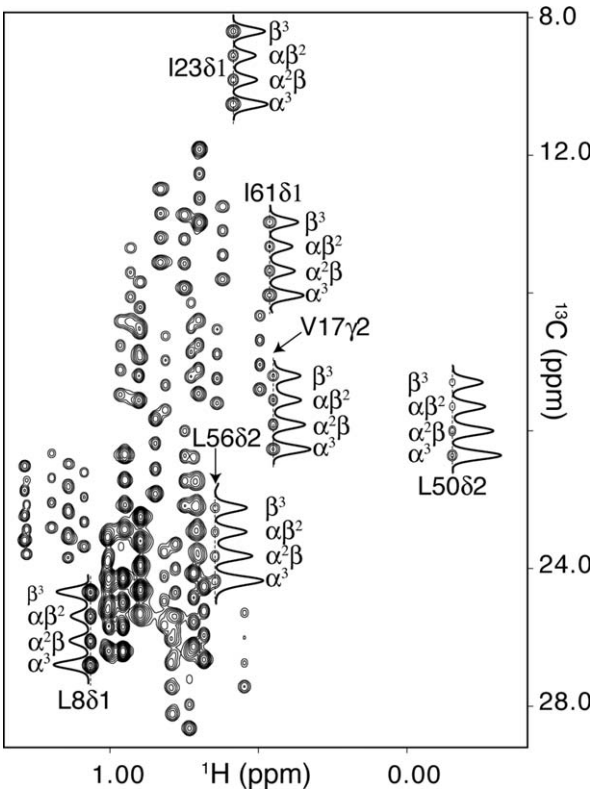

Figure 1. Constant time ^{13}C, ^{1}H HSQC spectrum of uniformly ^{15}N,^{13}C-labeled human ubiquitin recorded at a proton frequency of 700 MHz and a temperature of 275 K. The concentration of ubiquitin was 3.6 m*M* in 90%/10% H_2O/D_2O, containing 50 m*M* sodium phosphate at pH 6.8, 100 m*M* NaCl, and 0.1% NaN_3. The constant time duration and INEPT delays were set to 27.8 and 2 ms, respectively. The spectrum was recorded with 1024 and 128 complex points in the direct (t_2) and indirect (t_1) dimensions, respectively, with eight scans per t_1 increment. The $t_{1,max}$ and $t_{2,max}$ were 24.3 ms and 113 ms, respectively. Frequency discrimination in the indirectly detected dimension was achieved with the States-TPPI scheme.[43] The spectrum was processed with NMRPipe software.[44] 1D slices of selected quartets are illustrated together with the corresponding coherences for each peak in the multiplet.

Immediately clear from the measurement at 275 K (see Fig. 1), the peaks in the highlighted quartets are well resolved, despite the increase in τ_c accompanied with lowering the temperature. In addition, even at 275 K, a significant amount of motion is evident for the methyl groups of ubiquitin, especially for L8δ1 whose quartet approaches the ideal 3:1:1:3 intensity ratio.

For nearly 50% of all methyl groups in ubiquitin, Eq. (3) was used to calculate σ_{obs} at each of the 14 temperatures. The results are compiled in Supporting Information Table SI. For the remaining 28 methyl groups, either spectral overlap becomes problematic due to the chemical shift differences between methyl group carbons being similar to J_{CH}, $2J_{CH}$, or $3J_{CH}$[20] and/or strong coupling is present between the δ and γ carbons in leucine as reported for L15δ1, L43δ1, L50δ1, L56δ1, and L69δ2.[21] In addition, we only analyzed methyl groups whose quartets were not overlapped with other methyl group quartets over the entire temperature range (275–308 K).

As evident from the range of σ_{obs} at each temperature, the methyl groups exist in a wide array of environments. Variations in the mobility of the methyl group contribute to the observed differences in σ_{obs}. It should be noted that studying the temperature dependence of methyl group dynamics with deuterium relaxation studies,[17–19,26] though more time consuming, enables many more methyl groups to be analyzed due to significantly less spectral overlap. Nevertheless, with the wide availability of residue selective methyl group labeling,[27–29] which now even includes stereospecific selection of methyl groups,[30] we anticipate this approach being applicable to proteins larger than ubiquitin.

Quantification of methyl group dynamics in ubiquitin

The experimental CCR rate can be used to extract the methyl group order parameter (S^2_{axis}) by comparing σ_{obs} with the theoretical value of the CCR (σ_{rigid}) in the absence of local motions[20,25,31]:

$$S^2_{axis} = \frac{\sigma_{obs}}{\sigma_{rigid}} \quad (4)$$

$$\sigma_{rigid} = \frac{1}{45}\left(\frac{\mu_0 h \gamma_H \gamma_C}{8\pi^2 r^3_{CH}}\right)^2 \left(2\tau_c + \frac{3\tau_c}{2(1+(\omega_c\tau_c)^2)}\right) \quad (5)$$

where μ_0 is the permeability of a vacuum, h is the Planck constant, γ_H and γ_C are the gyromagnetic ratios of ^{1}H and ^{13}C, respectively, r_{CH} is the CH bond length, ω_C is the Larmor frequency of ^{13}C and τ_c is the rotational correlation time. S^2_{axis} is a dimensionless quantity utilized for describing the amplitude of motions for the methyl group.[25] Values for S^2_{axis} range from 0 to 1, where 1 represents a rigid methyl group and zero represents unrestricted local motion.

For determination of σ_{rigid} with Eq. (5), the methyl group C—H bond length (r_{CH}) was taken as 1.095 angstroms, tetrahedral geometry assumed and the τ_c of ubiquitin at each temperature is reported in Supporting Information Table SII. With σ_{rigid}, we calculated S^2_{axis} with Eq. (4) for all 14 temperatures, presented in the Supporting Information Table SII. Figure 2 illustrates the correlation of calculated S^2_{axis} at a selected set of temperatures. Readily apparent from the figure is the high degree of correlation for S^2_{axis} over these temperatures. For every pair-wise combination of S^2_{axis}, the Pearson correlation coefficient is $r \geq 0.98$. Since S^2_{axis} has a linear dependence on T, the high correlation between S^2_{axis} at all the temperatures suggests that uncertainties arising

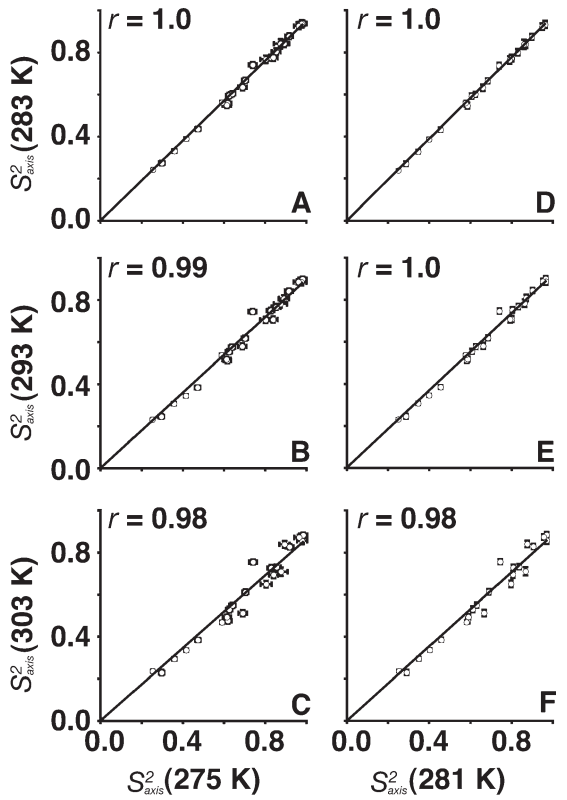

Figure 2. Correlations between methyl group order parameters (S^2_{axis}) of ubiquitin determined at multiple temperatures. (A) 283 K vs. 275 K, (B) 293 K vs. 275 K, (C) 303 K vs. 275 K, (D) 283 K vs. 281 K, (E) 293 K vs. 281 K, and (F) 303 K vs. 281 K. The solid line represents the best fit. The error bars for S^2_{axis} in both dimensions are included and in many cases are smaller than the symbol size. The Pearson correlation *r* is also shown.

from each experimental measurement are consistent over the entire data set. Figure 3(A) presents the correlation plot of S^2_{axis} values from CCR measurements versus S^2_{axis} extracted from the rates of multiple spin coherences involving ^2H in the methyl group, both at 303 K.[26] Figure 3(B) is the correlation plot of the currently reported S^2_{axis} at 301 K versus S^2_{axis} extracted from methyl group ^{13}C spin-lattice (T_1) relaxation rates and σ modulated by the one bond C—H coupling constant (J_{CH}) measured at 300 K.[21] For both comparisons, the Pearson correlation coefficient is high, 0.96 and 0.97, respectively. The agreement between S^2_{axis} obtained by three independent studies coupled with the high correlation for S^2_{axis} over the entire temperature range provides strong confirmation that the temperature dependence of S^2_{axis} can be studied using this method. It is important to point out that deviations from the diagonal most likely indicate small differences in experimental setup, such as sample conditions, slight temperature variations, and/or measurement error. Most importantly, we have significantly reduced the total amount of time required to obtain this information. With methods involving ^2H labeling of methyl groups,[17–19] R_1 and R_2 relaxation rates are typically measured in order to extract S^2_{axis} at one temperature. As for σ modulated by the one bond C—H coupling constant (J_{CH}), S^2_{axis} determined at one temperature needs a series of 2D constant time ^{13}C, ^1H HSQC measurements with increasing delay times.[21] However, with the present method, one temperature point requires only one 2D constant time ^{13}C, ^1H HSQC measurement.

Finally, the time-scale of motion encompassed by S^2_{axis} is faster than the τ_c of ubiquitin, describing ps to

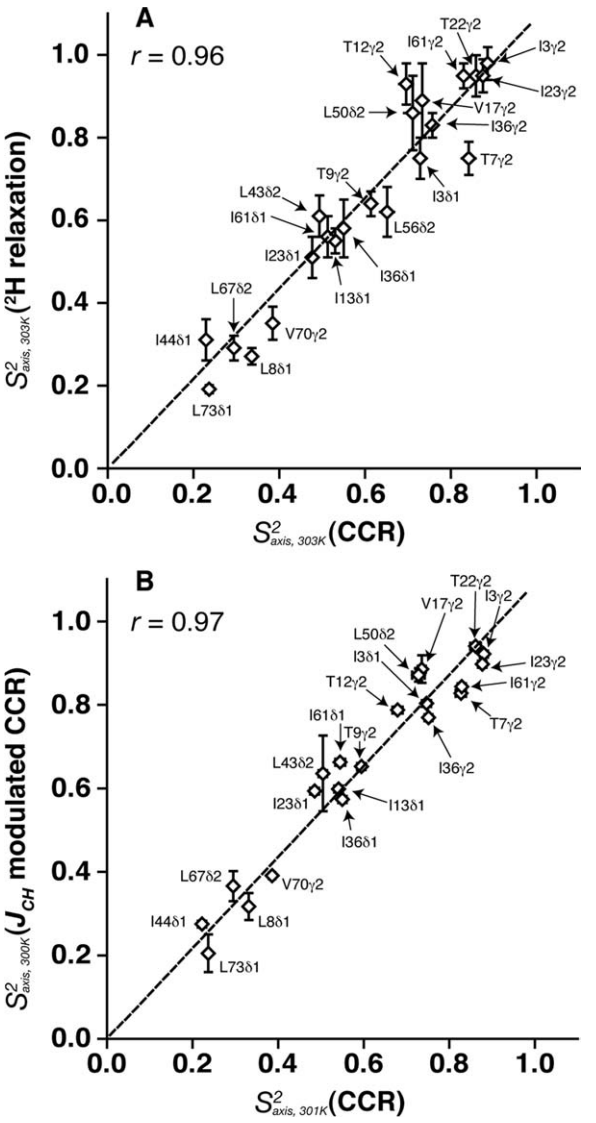

Figure 3. Comparison of S^2_{axis} in ubiquitin determined from different methods. A: Correlation between S^2_{axis} obtained from this study using dipolar CCR between CH bonds in the methyl group versus S^2_{axis} extracted from the rates of multiple spin coherences involving ^2H in the methyl group.[26] In both cases, S^2_{axis} was obtained at 303 K. B: Correlation between S^2_{axis} obtained at 301 K from the present study versus S^2_{axis} extracted at 300 K from methyl group ^{13}C spin-lattice (T_1) relaxation rates and dipolar CCR modulated by the one bond C—H coupling constant (J_{CH}).[21] In both figures, the dashed lines represent the best fit to the data. The error bars are included in both dimensions. The Pearson correlation *r* is also indicated in the figures.

Table I. *Thermal Coefficients Extracted from Methyl Group Order Parameters (S^2_{axis}) Within Ubiquitin*[a]

	κ (× 10^{-3} K^{-1})[b]	Λ[c]	C_p (J $K^{-1}mol^{-1}$)[d]
I3γ2	−2.9 ± 0.4	7.5 ± 1.4	52.7 ± 11.9[e]
I3δ1	−2.5 ± 0.4	3.2 ± 0.5	27.3 ± 4.5
T7γ2	−0.8 ± 0.5	1.0 ± 0.8	8.5 ± 7.9
L8δ1	−2.3 ± 0.2	1.4 ± 0.1	13.1 ± 1.1
T9γ2	−3.0 ± 0.3	2.7 ± 0.1	23.4 ± 2.8
T12γ2	−4.4 ± 0.4	4.8 ± 0.4	41.5 ± 4.9
I13δ1	−3.2 ± 0.3	2.5 ± 0.2	22.4 ± 2.3
V17γ2	−3.1 ± 0.4	4.0 ± 0.4	34.7 ± 4.3
T22γ2	−3.3 ± 0.5	8.1 ± 0.4	59.7 ± 14.1[e]
I23γ2	−2.3 ± 0.4	5.5 ± 1.1	43.9 ± 11.4[f]
I23δ1	−4.3 ± 0.4	3.1 ± 0.2	27.6 ± 2.6
I36γ2	0.1 ± 0.4	−0.8 ± 0.3	−6.9 ± 3.7
I36δ1	−2.8 ± 0.3	2.2 ± 0.2	19.8 ± 2.4
L43δ2	−3.6 ± 0.4	2.6 ± 0.2	23.4 ± 2.4
I44δ1	−2.6 ± 0.3	1.5 ± 0.2	14.8 ± 1.7
L50δ2	−5.4 ± 0.6	7.5 ± 0.6	64.5 ± 7.7
L56δ2	−5.2 ± 0.5	5.7 ± 0.4	49.3 ± 4.9
I61γ2	−2.5 ± 0.3	4.7 ± 0.6	39.5 ± 6.6
I61δ1	−5.7 ± 0.4	4.6 ± 0.3	40.4 ± 3.0
L67δ2	−2.1 ± 0.2	1.2 ± 0.1	11.8 ± 1.2
V70γ2	−2.3 ± 0.3	1.4 ± 0.1	13.4 ± 1.5
L73δ1	0.0 ± 0.1	0.2 ± 0.1	1.6 ± 0.7
Average	−2.9 ± 1.5	3.4 ± 2.4	28.5 ± 18.9

[a] All errors were determined from 500 Monte Carlo simulation runs.
[b] The temperature dependencies of S^2_{axis} ($\kappa = \frac{dS^2_{\text{axis}}}{dT}$) were obtained from the slope of a linear fit of S^2_{axis} versus temperature (T).[15]
[c] The characteristic thermal coefficient Λ was obtained from the slope of a linear fit of $(1 - \sqrt{S^2_{\text{axis}}})$ versus $\ln T$.[11]
[d] The heat capacities (C_p) were obtained from the slope of a linear fit of the conformational entropy (S_{conf}) versus $\ln T$,[34] where $S_{\text{conf}} = k_B N_A \left\{ \ln \pi \left[3 - \sqrt{1 + 8\sqrt{S^2_{\text{axis}}}} \right] \right\}$[8,9] k_B and N_A are the Boltzmann constant and Avogadro's number, respectively.
[e] For these methyl groups, only S^2_{axis} from temperatures between 283 and 308 K were used for the fitting procedure due to the requirement of $S^2_{\text{axis}} < 0.95$ for determining S_{conf}[8].
[f] For this methyl group, only S^2_{axis} from temperatures between 278 and 308 K were used for the fitting procedure due to the requirement of $S^2_{\text{axis}} < 0.95$ for determining of S_{conf}[8].

ns dynamics. An earlier study from our group has determined the methyl group RDC-based order parameters S^2_{RDC} for ubiquitin,[32] which reflect time-scales from ps to ms. When comparing the two sets of order parameters at 308 K, the average values of S^2_{axis} and S^2_{RDC} are 0.59 ± 0.21 and 0.43 ± 0.25, respectively, with a Pearson correlation coefficient of $r = 0.84$. Clearly, the methyl groups possess additional dynamics on a slower time-scale than encapsulated by S^2_{axis}.

Analysis of the temperature dependence of S^2_{axis} in ubiquitin

To quantify the temperature dependencies of S^2_{axis}, the thermal coefficient κ was taken from the linear fit of S^2_{axis} versus temperature $\left(\kappa = (dS^2_{\text{axis}}/dT)\right)$.[15] Table I and Figure 4 present the results of the fitting procedure. An overall decrease is observed in S^2_{axis} as the temperature increases from 275 to 308 K. The average value of κ is $-(2.9 \pm 1.5) \times 10^{-3}$ K^{-1}, which is quite comparable to the value of $-(2.6 \pm 1.1) \times 10^{-3}$ K^{-1} reported previously for ubiquitin over the larger temperature range of 278–328 K.[16] Furthermore, similar trends in the deviation of S^2_{axis} with temperature are also observed for calmodulin bound to a peptide.[15] Figure 5(A) illustrates the distribution of κ within ubiquitin (1UBQ).[33] The largest κ values are clustered around I61δ1, spatially near the N-terminus of ubiquitin, and progressively decrease toward the C-terminus of the protein.

The characteristic thermal coefficient $\Lambda = d \ln(1 - \sqrt{S^2_{\text{axis}}})/d \ln T$ relates the temperature dependencies of the generalized order parameter, in this case S^2_{axis}, to the characteristic temperature (T^*).[10,11] The term T^* describes the density of thermally accessible conformational states.[10] Table I presents the results for the determination of Λ, which correlates with κ (Pearson coefficients of $r = 0.7$). The average value of Λ (3.4 ± 2.4 compared with 2.3 ± 1.0 previously reported for ubiquitin over the larger temperature range of 278–328 K[16]) indicates that there is significant contributions from rotameric state dynamics.[14] In Figure 5(B), Λ is plotted on the structure of ubiquitin. As with κ, the largest values of Λ are located in the N-terminal region of ubiquitin. Toward the C-terminal region a progressive decline of Λ is visible.

Determination of the C_p from the temperature dependence of the conformational entropy

An approximate relationship between the conformational entropy (S_{conf}) and S^2_{axis} is

$$S_{\text{conf}} = k_B N_A \left\{ \ln \pi \left[3 - \sqrt{1 + 8\sqrt{S^2_{\text{axis}}}} \right] \right\}, \qquad (6)$$

where k_B is the Boltzmann constant and N_A is Avogadro's number.[8] The heat capacity (C_p) obtained from the temperature dependence of S_{conf} is defined as[34]

$$C_p = \frac{dS_{\text{conf}}}{d \ln T}. \qquad (7)$$

Table I presents the values of C_p for the methyl groups in ubiquitin for the temperature interval of 275–308 K. For 22 methyl groups in ubiquitin, we report an average C_p of 28.5 ± 18.9 J K^{-1} mol^{-1}. For the drkN SH3 domain, similar values for the methyl group C_p were obtained: 17 ± 12 J K^{-1} mol^{-1} and 33 ± 23 J K^{-1} mol^{-1} for the temperature intervals 287–303 K and 278–287 K, respectively.[9]

As measured by differential scanning calorimetry, the global C_p for ubiquitin was ~12.6 kJ K^{-1} mol^{-1} at 298 K.[35] In this study, the summation of all the individual methyl group C_p equals 626 J K^{-1} mol^{-1}. Keeping in mind that this value does not include the contributions of 28 additional methyl groups where C_p could not be determined, these results suggest that the total methyl group C_p makes a ~10% contribution to the total C_p of ubiquitin. It should be noted that a majority C_p can be determined from the primary sequence of proteins.[1] Since 16% (200 out of 1231) of all atoms in ubiquitin are from the methyl groups, the ~10% contribution for the methyl groups to the total ubiquitin C_p seems to be a reasonable estimate. Figure 5(C) presents the distribution of C_p in ubiquitin. The largest values of C_p, as with κ and Λ, are located spatially near the N-terminus of the protein, which is the part of the hydrophobic core of the protein.

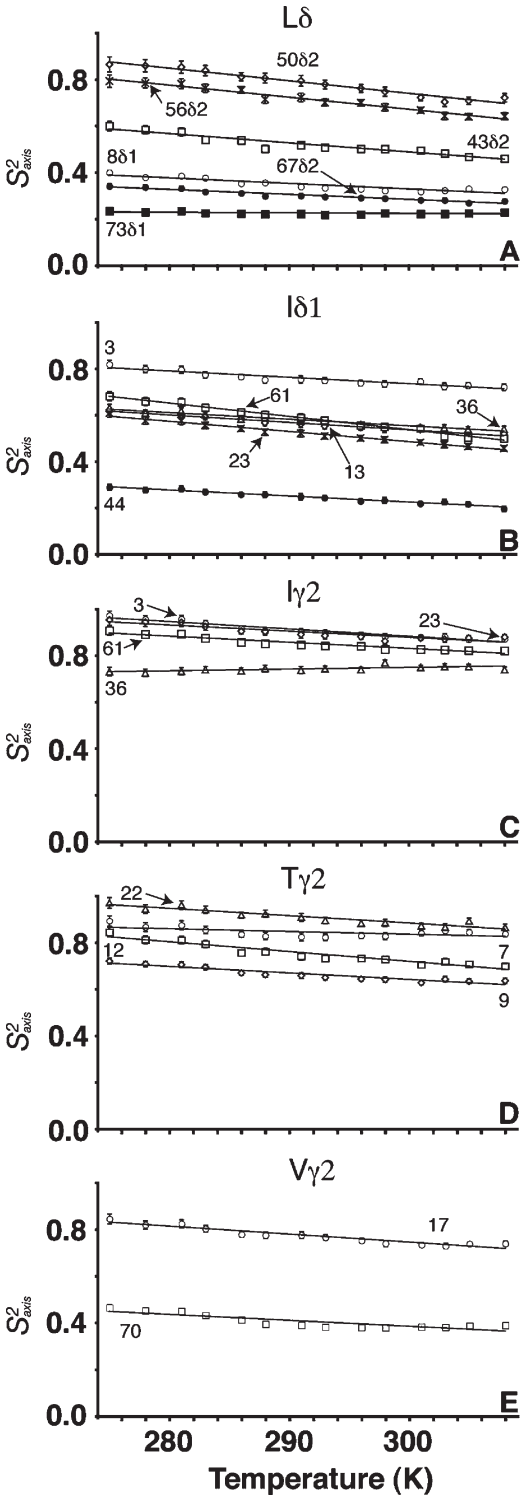

Insight into the thermal stability of ubiquitin from the distribution of thermal coefficients

A striking feature regarding the distribution of the thermal coefficients is the concentration of the largest values near the N-terminus of the protein. For these methyl groups to be located within the core of the protein may appear first at to be counterintuitive. Flexible regions tend to populate additional states more readily (especially upon an increase in thermal energy) and thus, would potentially possess larger than average C_p values. In addition, several studies indicate that the N-terminal region of ubiquitin, specifically the α-helix and the turn between β-strands 1 and 2, is quite resilient to temperature fluctuations[36,37] and comprises the core structural elements that form first during ubiquitin folding.[38,39] However, investigations into the temperature dependence of NH order parameters for several thermo-stable proteins reveal some of the larger C_p values to be located within the more rigid regions of secondary structure.[11–13] Furthermore, the magnitude of C_p depends on the change in S_{conf} [see Eq. (7)], and, as calculated by three independent groups,[7,8,11] the steepest change for S_{conf} occurs as the order parameter, S^2, varies between 0.7 and 0.95. Perhaps the high melting temperature of ~363 K for ubiquitin[35] and other thermo-stabile proteins can be attributed in part to the relatively large local C_p of the methyl groups and NH bonds in the folded proteins reducing the magnitude of ΔC_p upon unfolding.

Figure 4. Temperature dependence of S^2_{axis} in ubiquitin ($\kappa = dS^2_{axis}/dT$). All data were fit with a linear regression line in order to obtain κ (solid line).[15] For many of the data points, the error bars are smaller than the symbol size. A: Plot of the temperature dependence of S^2_{axis} for the following leucine δ methyl groups: 8δ1 (○), 43δ2 (□), 50δ2 (◇), 56δ2 (×), 67δ2 (●), and 73δ1 (■). B: Plot of the temperature dependence of S^2_{axis} for the following isoleucine δ1 methyl groups: 3 (○), 13 (◇), 23 (×), 36 (△), 44 (●), and 61 (□). C: Plot of the temperature dependence of S^2_{axis} for the following isoleucine γ2 methyl groups: 3 (○), 23 (◇), 36 (△), and 61 (□). D: Plot of the temperature dependence of S^2_{axis} for the following threonine γ2 methyl groups: 7 (○), 9 (◇), 12 (□), and 22 (△). E: Plot of the temperature dependence of S^2_{axis} for the following valine γ2 methyl groups: 17 (○) and 70 (□).

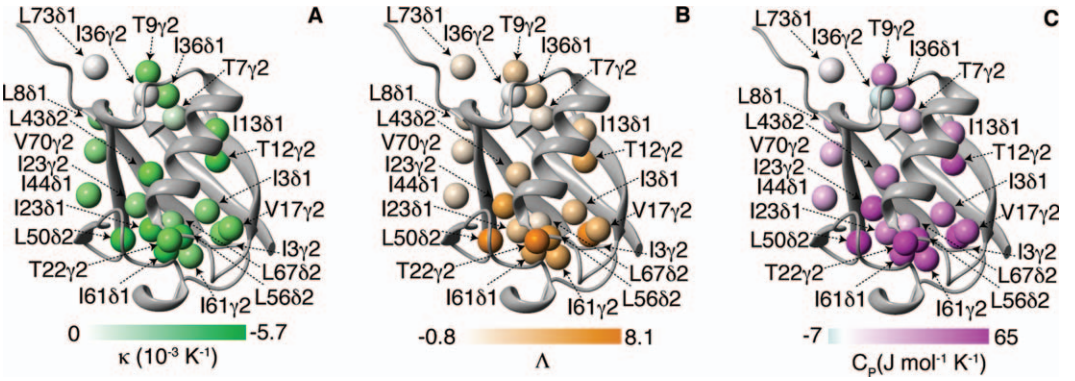

Figure 5. Location of the calculated thermal coefficients for methyl groups in ubiquitin (1UBQ).[33] A: Distribution of κ. B: Distribution of the characteristic thermal coefficient Λ, which was obtained from a linear fit of $(1-\sqrt{S^2_{\text{axis}}})$ versus ln T.[11] C: Distribution of the heat capacity (C_p), which was obtained from a linear fit of the conformational entropy (S_{conf}) versus ln T,[34] where $S_{\text{conf}} = k_B N_A \left\{ \ln \pi \left[3 - \sqrt{1 + 8\sqrt{S^2_{\text{axis}}}} \right] \right\}$[8,9]. k_B and N_A are the Boltzmann constant and Avogadro's number, respectively. Spheres represent the carbon atom of the indicated methyl group. The color gradient is employed for identifying the magnitude of the specified thermal parameter. The figures were created with the program MOLMOL.[46]

One methyl group possesses a slightly negative C_p, I36γ2. Two other studies have reported negative C_p for NH bonds located in secondary structural regions.[12,15] Enhancements in the strength of hydrophobic interactions with increasing temperature were given as a possible explanation for this phenomenon.[40] In the case of I36γ2, previous work has demonstrated that the hydrophobic interaction between the side chain of I36 and I30 at the C-terminus of the α-helix is important for the stability of ubiquitin.[41] Thus, the negative C_p signifying a decrease in the flexibility and a reduction in the available conformational space for this methyl group may be related to the strengthening of this important interaction with increasing temperature.

Conclusion

In this study, we analyzed the temperature dependence for the methyl group order parameters in ubiquitin. With the requirement of only one 2D constant time ^{13}C, ^{1}H HSQC measurement without decoupling of ^{1}H during ^{13}C-chemical shift evolution, we have significantly reduced the total amount of experimental time required to obtain this information. From these experiments, the extracted thermal coefficients provide a glimpse into the location of ubiquitin thermo-stability near the N-terminus of the protein. Clearly, methyl groups contribute quite appreciably to the total heat capacity of ubiquitin, as well as of other proteins,[9,15] through the regulation of local conformational entropy. Taken together with the temperature dependence of NH order parameters, a per residue gauge of local protein thermodynamics offers a powerful complement to the already well-established methods for determining global thermodynamic parameters in proteins.

Materials and Methods

NMR spectroscopy and processing

Uniformly ^{15}N,^{13}C-labeled human ubiquitin was expressed and purified as described previously.[42] For the NMR measurements, a 3.6 mM sample of the protein was prepared in 350 μL of 50 mM sodium phosphate buffer, 100 mM NaCl, 0.1% NaN_3, and pH 6.8 in 10% D_2O/90% H_2O. A series of 2D constant time ^{13}C, ^{1}H HSQCs without decoupling of ^{1}H during ^{13}C-chemical shift evolution were measured at 14 temperature points: 275, 278, 281, 283, 286, 288, 291, 293, 296, 298, 301, 303, 305, and 308 K. All NMR experiments were performed in succession on a 700 MHz Avance-III Bruker spectrometer equipped with a triple resonance probe head. The constant time duration and INEPT delays were set to 27.8 and 2 ms, respectively. The spectrum was recorded with 1024 and 128 complex points in the direct (t_2) and indirect (t_1) dimensions, respectively, with eight scans per t_1 increment. The $t_{1,\max}$ and $t_{2,\max}$ were 24.3 ms and 113 ms, respectively. Frequency discrimination in the indirectly detected dimension was achieved with the States-TPPI scheme.[43] Each measurement required 59 min.

All time domain data were processed in the same manner with NMRPipe software.[44] The data were zero-filled to 8 and 16 k in t_1 and t_2, respectively. After implementing a time domain solvent correction, a sine-bell window function was applied in the direct dimension, followed by Fourier transformation of t_2. For the indirect dimension, a mirror image linear prediction algorithm was used to increase the resolution in t_1. Next, a Gaussian window function was employed followed by Fourier transformation of t_1. Finally, a polynomial baseline correction in the frequency domain was applied in the direct dimension.

Methods for error determination

The intensities of each peak in the quartet were taken from the program CARA[45] and the dipolar-dipolar CCR rates (σ_{obs}) were calculated according to Eq. (3). To determine the errors in σ_{obs}, the noise levels (q) for each measurement were estimated using NMRPipe and the error ($\Delta\sigma_{obs}$) was obtained from the following relation,

$$\Delta\sigma_{obs} = \frac{q}{8\Delta}\left(\frac{1}{I_{\alpha^3}} + \frac{1}{I_{\alpha^2\beta}} + \frac{1}{I_{\alpha\beta^2}} + \frac{1}{I_{\beta^3}}\right), \quad (8)$$

where Δ is the length of the constant time period and I_i is the intensity of each peak in the quartet ($i = \alpha^3, \alpha^2\beta, \alpha\beta^2$ or β^3). For the methyl group order parameters (S^2_{axis}), the errors (ΔS^2_{axis}) were calculated by propagating the error from $\Delta\sigma_{obs}$ using the equation,

$$\Delta S^2_{axis} = \frac{\Delta\sigma_{obs}}{\sigma_{rigid}}, \quad (9)$$

where σ_{rigid} is derived from Eq. (5). Finally, the errors in the conformational entropy (ΔS_{conf}) were determined by propagating the error from ΔS^2_{axis},

$$\Delta S_{conf} = 4k_B N_A A\left|\frac{1}{(3-B)B}\right|, \quad (10)$$

where

$$A = \frac{\Delta S^2_{axis}}{2\sqrt{S^2_{axis}}}, \quad (11)$$

$$B = \sqrt{1 + 8\sqrt{S^2_{axis}}}, \quad (12)$$

k_B is the Boltzmann constant and N_A is Avogadro's number. To estimate the error in the temperature dependency of $S^2_{axis}(\kappa = \frac{dS^2_{axis}}{dT})$, the characteristic thermal coefficient ($\Lambda = \frac{d\ln(1-\sqrt{S^2_{axis}})}{d\ln T}$), and the heat capacity ($C_p = \frac{dS_{conf}}{d\ln T}$), Monte Carlo simulations on 500 randomly generated data sets were performed.

References

1. Gomez J, Hilser VJ, Xie D, Freire E (1995) The heat-capacity of proteins. Proteins 22:404–412.
2. Prabhu NV, Sharp KA (2005) Heat capacity in proteins. Ann Rev Phys Chem 56:521–548.
3. Kay LE, Torchia DA, Bax A (1989) Backbone dynamics of proteins as studied by ^{15}N inverse detected heteronuclear NMR-spectroscopy-application to Staphylococcal nuclease. Biochemistry 28:8972–8979.
4. Lipari G, Szabo A (1982) Model-free approach to the interpretation of nuclear magnetic-resonance relaxation in macromolecules. 1. Theory and range of validity. J Am Chem Soc 104:4546–4559.
5. Lipari G, Szabo A (1982) Model-free approach to the interpretation of nuclear magnetic-resonance relaxation in macromolecules. 2. Analysis of experimental results. J Am Chem Soc 104:4559–4570.
6. Akke M, Bruschweiler R, Palmer AG (1993) NMR order parameters and free-energy-an analytical approach and its application to cooperative Ca^{2+} binding by calbindin-D(9k). J Am Chem Soc 115:9832–9833.
7. Li ZG, Raychaudhuri S, Wand AJ (1996) Insights into the local residual entropy of proteins provided by NMR relaxation. Protein Sci 5:2647–2650.
8. Yang DW, Kay LE (1996) Contributions to conformational entropy arising from bond vector fluctuations measured from NMR-derived order parameters: Application to protein folding. J Mol Biol 263:369–382.
9. Yang DW, Mok YK, Forman-Kay JD, Farrow NA, Kay LE (1997) Contributions to protein entropy and heat capacity from bond vector motions measured by NMR spin relaxation. J Mol Biol 272:790–804.
10. Mandel AM, Akke M, Palmer AG (1996) Dynamics of ribonuclease H: Temperature dependence of motions on multiple time scales. Biochemistry 35:16009–16023.
11. Vugmeyster L, Trott O, McKnight CJ, Raleigh DP, Palmer AG (2002) Temperature-dependent dynamics of the villin headpiece helical subdomain, an unusually small thermostable protein. J Mol Biol 320:841–854.
12. Led JJ, Vinther JM, Kristensen SM (2011) Enhanced stability of a protein with increasing temperature. J Am Chem Soc 133:271–278.
13. Stone MJ, Seewald MJ, Pichumani K, Stowell C, Tibbals BV, Regan L (2000) The role of backbone conformational heat capacity in protein stability: Temperature dependent dynamics of the B1 domain of Streptococcal protein G. Protein Sci 9:1177–1193.
14. Wand AJ, Lee AL (2001) Microscopic origins of entropy, heat capacity and the glass transition in proteins. Nature 411:501–504.
15. Lee AL, Sharp KA, Kranz JK, Song XJ, Wand AJ (2002) Temperature dependence of the internal dynamics of a calmodulin-peptide complex. Biochemistry 41:13814–13825.
16. Wand AJ, Song XJ, Flynn PF, Sharp KA (2007) Temperature dependence of fast dynamics in proteins. Biophys J 92:L43–L45.
17. Muhandiram DR, Yamazaki T, Sykes BD, Kay LE (1995) Measurement of ^{2}H T_1 and $T_{1\rho}$ relaxation-times in uniformly ^{13}C-labeled and fractionally ^{2}H-labeled proteins in solution. J Am Chem Soc 117:11536–11544.
18. Liao X, Long D, Li DW, Brüschweiler R, Tugarinov V (2012) Probing side-chain dynamics in proteins by the measurement of nine deuterium relaxation rates per methyl group. J Phys Chem B 116:606–620.
19. Millet O, Muhandiram DR, Skrynnikov NR, Kay LE (2002) Deuterium spin probes of side-chain dynamics in proteins. 1. Measurement of five relaxation rates per deuteron in ^{13}C-labeled and fractionally ^{2}H-enriched proteins in solution. J Am Chem Soc 124:6439–6448.
20. Liu WD, Zheng Y, Cistola DP, Yang DW (2003) Measurement of methyl ^{13}C-^{1}H cross-correlation in uniformly ^{13}C, ^{15}N-labeled proteins. J Biomol NMR 27:351–364.
21. Zhang X, Sui XG, Yang DW (2006) Probing methyl dynamics from ^{13}C autocorrelated and cross-correlated relaxation. J Am Chem Soc 128:5073–5081.
22. Kay LE, Bull TE, Nicholson LK, Griesinger C, Schwalbe H, Bax A, Torchia DA (1992) The measurement of heteronuclear transverse relaxation-times in Ax3 spin systems via polarization-transfer techniques. J Magn Reson 100:538–558.
23. Müller N, Bodenhausen G, Ernst RR (1987) Relaxation-induced violations of coherence transfer selection-

rules in nuclear-magnetic-resonance. J Magn Reson 75: 297–334.
24. Tugarinov V, Hwang PM, Ollerenshaw JE, Kay LE (2003) Cross-correlated relaxation enhanced $^{1}H—^{13}C$ NMR spectroscopy of methyl groups in very high molecular weight proteins and protein complexes. J Am Chem Soc 125:10420–10428.
25. Kay LE, Torchia DA (1991) The effects of dipolar cross-correlation on ^{13}C methyl-carbon T_1, T_2, and NOE measurements in macromolecules. J Magn Reson 95: 536–547.
26. Lee AL, Flynn PF, Wand AJ (1999) Comparison of ^{2}H and ^{13}C NMR relaxation techniques for the study of protein methyl group dynamics in solution. J Am Chem Soc 121:2891–2902.
27. Goto NK, Gardner KH, Mueller GA, Willis RC, Kay LE (1999) A robust and cost-effective method for the production of Val, Leu, Ile (δ1) methyl-protonated ^{15}N-, ^{13}C-, ^{2}H-labeled proteins. J Biomol NMR 13:369–374.
28. Godoy-Ruiz R, Guo C, Tugarinov V (2010) Alanine methyl groups as NMR probes of molecular structure and dynamics in high-molecular-weight proteins. J Am Chem Soc 132:18340–18350.
29. Ruschak AM, Velyvis A, Kay LE (2010) A simple strategy for ^{13}C, ^{1}H labeling at the Ile-γ2 methyl position in highly deuterated proteins. J Biomol NMR 48:129–135.
30. Gans P, Hamelin O, Sounier R, Ayala I, Dura MA, Amero CD, Noirclerc-Savoye M, Franzetti B, Plevin MJ, Boisbouvier J (2010) Stereospecific isotopic labeling of methyl groups for NMR spectroscopic studies of high-molecular-weight proteins. Angew Chem Int Ed Engl 49:1958–1962.
31. Lee D, Hilty C, Wider G, Wüthrich K (2006) Effective rotational correlation times of proteins from NMR relaxation interference. J Magn Reson 178:72–76.
32. Fares C, Lakomek NA, Walter KFA, Frank BTC, Meiler J, Becker S, Griesinger C (2009) Accessing ns-μs side chain dynamics in ubiquitin with methyl RDCs. J Biomol NMR 45:23–44.
33. Vijaykumar S, Bugg CE, Cook WJ (1987) Structure of ubiquitin refined at 1.8 Å resolution. J Mol Biol 194: 531–544.
34. Privalov PL, Gill SJ (1988) Stability of protein-structure and hydrophobic interaction. Adv Protein Chem 39:191–234.
35. Wintrode PL, Makhatadze GI, Privalov PL (1994) Thermodynamics of ubiquitin unfolding. Proteins 18:246–253.
36. Wand AJ, Babu CR, Hilser VJ (2004) Direct access to the cooperative substructure of proteins and the protein ensemble via cold denaturation. Nat Struct Mol Biol 11:352–357.
37. Grzesiek S, Cordier F (2002) Temperature-dependence properties as studied by of protein hydrogen bond high-resolution NMR. J Mol Biol 317:739–752.
38. Jackson SE, Went HM (2005) Ubiquitin folds through a highly polarized transition state. Protein Eng Des Sel 18:229–237.
39. Brutscher B, Brüschweiler R, Ernst RR (1997) Backbone dynamics and structural characterization of the partially folded A state of ubiquitin by ^{1}H, ^{13}C, and ^{15}N nuclear magnetic resonance spectroscopy. Biochemistry 36:13043–13053.
40. Baldwin RL (1986) Temperature-dependence of the hydrophobic interaction in protein folding. Proc Natl Acad Sci USA 83:8069–8072.
41. Thomas ST, Makhatadze GI (2000) Contribution of the 30/36 hydrophobic contact at the C-terminus of the alpha-helix to the stability of the ubiquitin molecule. Biochemistry 39:10275–10283.
42. Handel TM, Johnson EC, Lazar GA, Desjarlais JR (1999) Solution structure and dynamics of a designed hydrophobic core variant of ubiquitin. Structure 7:967–976.
43. Marion D, Ikura M, Tschudin R, Bax A (1989) Rapid recording of 2D NMR-spectra without phase cycling: Application to the study of hydrogen-exchange in proteins. J Magn Reson 85:393–399.
44. Delaglio F, Grzesiek S, Vuister GW, Zhu G, Pfeifer J, Bax A (1995) Nmrpipe-a multidimensional spectral processing system based on Unix pipes. J Biomol NMR 6:277–293.
45. Keller R (2004) Computer Aided Resonance Assignment. http://cara.nmr.ch/.
46. Koradi R, Billeter M, Wüthrich K (1996) MOLMOL: A program for display and analysis of macromolecular structures. J Mol Graph 14:51–55.